Assembly of the PtdIns 4-kinase Stt4 complex at the plasma membrane requires Ypp1 and Efr3

Dan Baird,[1,2] Chris Stefan,[1,2] Anjon Audhya,[3] Sabine Weys,[1,2] and Scott D. Emr[1,2]

[1]Weill Institute for Cell and Molecular Biology and [2]Department of Molecular Biology and Genetics, Cornell University, Ithaca, NY 14853
[3]Department of Biomolecular Chemistry, University of Wisconsin-Madison, Madison, WI 53706

The phosphoinositide phosphatidylinositol 4-phosphate (PtdIns4P) is an essential signaling lipid that regulates secretion and polarization of the actin cytoskeleton. In *Saccharomyces cerevisiae*, the PtdIns 4-kinase Stt4 catalyzes the synthesis of PtdIns4P at the plasma membrane (PM). In this paper, we identify and characterize two novel regulatory components of the Stt4 kinase complex, Ypp1 and Efr3. The essential gene *YPP1* encodes a conserved protein that colocalizes with Stt4 at cortical punctate structures and regulates the stability of this lipid kinase. Accordingly, Ypp1 interacts with distinct regions on Stt4 that are necessary for the assembly and recruitment of multiple copies of the kinase into phosphoinositide kinase (PIK) patches. We identify the membrane protein Efr3 as an additional component of Stt4 PIK patches. Efr3 is essential for assembly of both Ypp1 and Stt4 at PIK patches. We conclude that Ypp1 and Efr3 are required for the formation and architecture of Stt4 PIK patches and ultimately PM-based PtdIns4P signaling.

Introduction

Cellular membranes are structured bilayers consisting of lipid and protein that define the boundaries of the cell and its organelles. Besides providing support and containment, membrane composition denotes organelle identity and transmits cellular signals. Among the various lipids incorporated into the membrane, inositol-containing phospholipids are ideally suited for transmitting signals because their inositol head group can be reversibly phosphorylated at three different hydroxyl positions. An array of kinases and phosphatases regulates phosphatidylinositol phosphate (PIP) signaling by controlling inositol head group phosphorylation to efficiently mediate the levels and location of specific PIPs. Proteins are able to recognize these phosphorylated head groups through specific modular domains (e.g., PH, PX, FYVE, or ENTH, etc.) and transmit this information throughout the cell (Lemmon, 2003). Naturally, the importance of PIP signaling is critical to a host of cellular processes ranging from receptor signaling pathways to regulation of actin cytoskeleton dynamics and vesicle trafficking (De Camilli et al., 1996; Odorizzi et al., 2000; Simonsen et al., 2001; Di Paolo and De Camilli, 2006).

The yeast *Saccharomyces cerevisiae* has proven useful as a genetic model system to study PIP signaling pathways because several of the lipid kinases, lipid phosphatases, and effectors are well conserved (Odorizzi et al., 2000). Each kinase or phosphatase localizes to a distinct region or organelle in the cell to control the levels and location of its corresponding phosphoinositide. Stt4, the yeast homologue to the human type III phosphatidylinositol (PtdIns) 4-kinase PtdIns(4)KIIIα, is essential in yeast and localizes to punctate dots on the plasma membrane (PM; Audhya and Emr, 2002). The other essential yeast PtdIns 4-kinase, Pik1, localizes to the Golgi and acts independently of Stt4 function (Hama et al., 1999; Walch-Solimena and Novick, 1999; Audhya et al., 2000; Strahl et al., 2005). The phosphatidylinositol 4-phosphate (PtdIns4P) generated by either of these kinases is turned over by the Sac1 domain–containing proteins Sac1, Sjl2, and Sjl3 (Guo et al., 1999; Foti et al., 2001). Among these three proteins, Sac1 has been demonstrated to be the PtdIns 4-phosphatase primarily responsible for metabolizing Stt4-generated PtdIns4P at the PM (Foti et al., 2001). Stt4 has been indirectly implicated in regulation of the cell cycle (Muhua et al., 1998), lipid metabolism (Voelker, 2005; Tabuchi et al., 2006), actin cytoskeleton dynamics, and activation

D. Baird and C. Stefan contributed equally to this paper.

Correspondence to Scott D. Emr: sde26@cornell.edu

Abbreviations used in this paper: FPLC, fast protein liquid chromatography; PIP, phosphatidylinositol phosphate; PIK, phosphoinositide kinase; PM, plasma membrane; PtdIns, phosphatidylinositol; PtdIns4P, phosphatidylinositol 4-phosphate; RBO, rolling blackout; TPR, tetratricopeptide repeat.

The Rockefeller University Press $30.00
J. Cell Biol. Vol. 183 No. 6 1061–1074
www.jcb.org/cgi/doi/10.1083/jcb.200804003

of a MAPK pathway (Audhya and Emr, 2002). Despite the obvious importance for Stt4 and its lipid product, PtdIns4P, the precise regulation of Stt4 activity at the PM remains poorly understood.

This study describes the analysis of a unique cortical structure, Stt4-containing phosphoinositide kinase (PIK) patches. Previous work has demonstrated that both the PM-localized lipid kinases, Stt4 and Mss4, cluster into distinct cortical structures (Audhya and Emr, 2002). Furthermore, mammalian lipid kinases often localize to patches at sites of receptor-mediated signaling or membrane attachment to the extracellular matrix (Honda et al., 1999; Ling et al., 2003; Heck et al., 2007). Although PIK patches seem to be a widely adopted structure, it is unclear why cells need to maintain these arrangements. In this paper, we focus on Stt4 PIK patches and anticipate that common themes regarding these structures may emerge.

We identify two novel components of the Stt4 PIK patch: Ypp1 and Efr3. Ypp1 is an essential protein that directly contacts distinct sites on Stt4 to organize and stabilize PIK patches at the PM. Ypp1 and Stt4 colocalize on the PM to form the core of a large Stt4 complex visualized as punctate patches. Loss of Ypp1 from this complex mislocalizes Stt4 and results in the subsequent degradation of the lipid kinase. Efr3 likewise localizes with Ypp1 at Stt4 PIK patches, physically interacts with Ypp1, and is necessary for assembly of the PIK patch components Stt4 and Ypp1 at the PM. Consequently, cells lacking either Ypp1 or Efr3 fail to assemble the Stt4 PIK patch and fail to maintain proper PtdIns4P levels.

Results

Initial characterization of the Stt4 PIK patch

Using a three-dimensional reconstruction of z stacks from cells expressing an N-terminally tagged *GFP-STT4* construct, we have been able to estimate the number of Stt4 PIK patches on the PM of an individual cell as shown in Video 1 (available at http://www.jcb.org/cgi/content/full/jcb.200804003/DC1). The three-dimensional reconstruction of the cells is a representative sample of several previously analyzed populations. The fluorescence data indicate that each cell has ∼20–25 regions of dense fluorescence corresponding to a cluster of GFP-Stt4 within the PIK patch. Additionally, coimmunoprecipitation of HA-Stt4 with GFP-Stt4 from cells coexpressing the two epitope–tagged Stt4 proteins demonstrates that these proteins form a physical interaction (Fig. S1 A). Therefore, we believe the dense fluorescent cluster of GFP-Stt4 represents an oligomer of Stt4 at the PIK patch site. With the understanding that roughly 850 Stt4 molecules populate the average cell (Ghaemmaghami et al., 2003) and that the plasmid-expressed GFP-Stt4 fusion is maintained at the same concentration as wild-type Stt4 (Audhya and Emr, 2002), we can estimate that each Stt4 PIK patch contains ∼30 Stt4 molecules. This molecular abundance of Stt4 at a PIK patch corroborates well with the fluorescence intensity of a PIK patch measured against a known standard (Fig. S1 B). Thus, these results suggest that multiple copies of Stt4 oligomerize at PIK patches.

Identification of a novel component of the Stt4 PIK patch

To understand Stt4 PIK patch assembly and regulation, we sought novel Stt4-interacting partners. We examined several candidate PtdIns 4-kinase regulators by experimentally testing the various Stt4-interacting proteins cataloged in the *Saccharomyces* Genome Database and identified one uncharacterized essential protein: YGR198w (recently named Ypp1 [Flower et al., 2007]). This interaction was originally published by Hazbun et al. (2003), who isolated Ypp1 and corresponding binding partners through tandem affinity purification and subsequent mass spectrometry to identify Stt4 as the primary binding partner. To determine the localization of Ypp1 in live yeast cells, the sequence encoding GFP was integrated at the 3′ end of Ypp1's chromosomal locus to generate Ypp1-GFP (Fig. 1 A). Similar to GFP-Stt4 (Audhya and Emr, 2002), Ypp1-GFP localized to several punctate structures on the periphery of the cell with a majority of these patches concentrated in the mother cell. Furthermore, strong colocalization of Ypp1-mCherry with GFP-Stt4 on these punctate patches suggests they reside at the same cortical structure on the PM (Fig. 1 B).

Primary sequence analysis of Ypp1 reveals two separate tetratricopeptide repeat (TPR) domains as its only recognizable structural motif. TPR domains exist in nearly all organisms and have been shown to mediate a variety of protein–protein interactions (for review see D'Andrea and Regan, 2003). Furthermore, *YPP1* homologues are evident in several species; in humans, the closest homologue is *TTC7a* (TPR domain 7A; Fig. 1 C). Despite their similar sequence structure, however, *TTC7a* is not able to rescue the inviability of *ypp1Δ* yeast (unpublished data).

Stt4–Ypp1 PIK patches are static structures separate from other PM-based components

Stt4–Ypp1 PIK patches have been shown to be separate structures from Mss4 PIK patches (Audhya and Emr, 2002). However, it has been hypothesized that the Ypp1 PM structures are cortical actin patches because of their similar distribution (Flower et al., 2007). This seems unlikely as we found no significant colocalization of Abp1–monomeric RFP, a known component of cortical actin structures enriched in the bud (Stefan et al., 2005), with Ypp1-GFP or GFP-Stt4. Also, treatment with latrunculin A has no effect on the localization or dynamics of Stt4–Ypp1 PIK patches (Fig. S2 A, available at http://www.jcb.org/cgi/content/full/jcb.200804003/DC1). We examined whether the distribution of Stt4–Ypp1 PIK patches show similarity to another PM localized structure: Pil1-based eisosomes (Walther et al., 2006). Pil1-mCherry and GFP-Ypp1 show very limited colocalization (Fig. S2 B). Furthermore, GFP-Ypp1 localizes normally in *pil1Δ* cells (unpublished data). These findings show that Stt4 PIK patches and eisosomes are distinct organizational units of the PM.

Subsequently, we studied the dynamics of Stt4 and Ypp1 at PIK patches and compared it to the Stt4 product PtdIns4P. Fig. 2 A is a fluorescent image with the corresponding kymograph of GFP-Stt4 and Ypp1-GFP. Unlike cortical actin patches

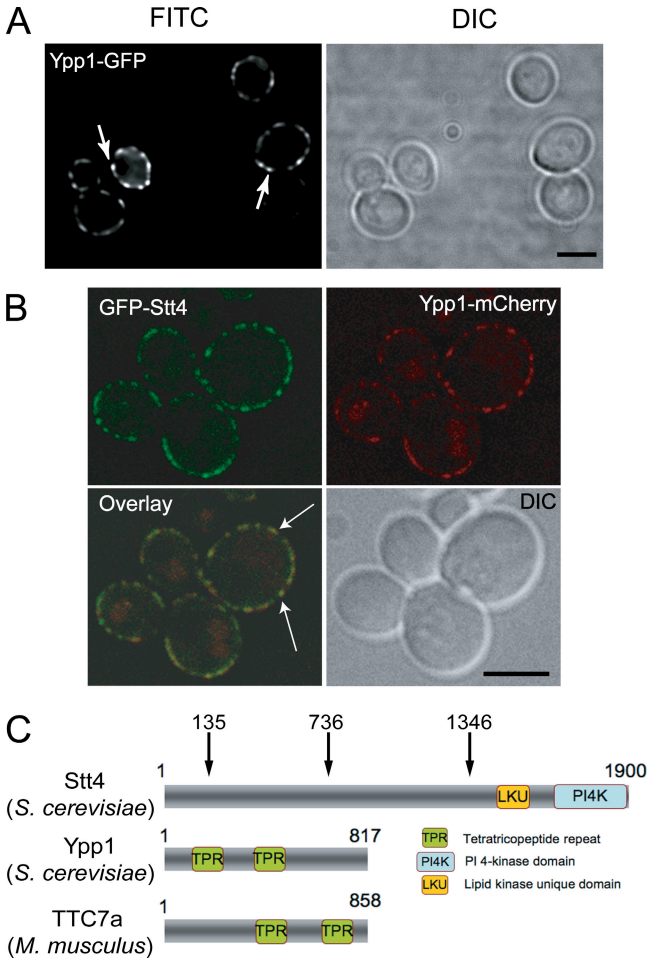

Figure 1. **Ypp1 colocalizes with Stt4 at static cortical structures at the PM.** (A) Cells expressing Ypp1-GFP were grown at 26°C and examined by fluorescence microscopy. Cells shown are representative of over 200 cells observed. Arrows show regions of highly concentrated Ypp1-GFP. Bar, 4 µm. (B) Cells coexpressing GFP-Stt4 and Ypp1-mCherry were grown at 26°C and examined by confocal microscopy. As previously reported (Audhya and Emr, 2002), GFP-Stt4 localizes to cortical patches on the PM (top left) and with a similar distribution as Ypp1-mCherry (top right). An overlay of the two images (bottom left) shows overlap of the fluorescent patches. Arrows indicate regions of the most conspicuous colocalization. Bar, 4 µm. (C) Schematic representation of Stt4, Ygr198w (Ypp1), and the Ypp1 human homologue TTC7a (available from GenBank/EMBL/DDBJ under accession no. NM_020458). Stt4 is a 215-kD protein with a lipid kinase unique domain (LKU) and a PtdIns 4-kinase domain (PI4K) as its only recognizable motifs. Ypp1 is a 95-kD protein encompassing multiple TPR domains and with conserved homologues in higher species. The schematics are not to scale.

(Kaksonen et al., 2005), GFP-Stt4 PIK patches are stable over the course of 3 min. To test whether the Stt4 molecules residing in these patches were also static instead of dynamically exchanging, we performed FRAP on a region of the PM (Fig. 2 B and Video 2, available at http://www.jcb.org/cgi/content/full/jcb.200804003/DC1). 3 min after photobleaching a PIK patch–rich region of the PM, none of the fluorescence had recovered. This is in stark contrast to the Stt4 product PtdIns4P as observed with a PtdIns4P reporter, GFP-2xPH^{Osh2} (Yu et al., 2004). After photobleaching a PtdIns4P-rich region of the PM, the fluorescence of the GFP-2xPH^{Osh2} reporter recovers rapidly (Fig. 2 B and Video 3).

Ypp1 directly interacts with Stt4

We next examined the contribution of Ypp1 on the interesting characteristics of Stt4 PIK patches. First, we determined if the two proteins interacted. A yeast strain expressing HA-tagged Ypp1 and either GFP-tagged Stt4 or GFP alone was detergent solubilized and immunoprecipitated using a GFP antibody. HA-Ypp1 showed no interaction with GFP alone, but a significant interaction with GFP-Stt4 (Fig. 2 C). Subsequent in vitro pulldown experiments using GST-tagged regions of Stt4 generated from *Escherichia coli* identified at least two separate Ypp1-interacting regions. Both the N-terminal third of Stt4 (represented by amino acids 1–736) and a central region (represented by amino acids 736–1346) both bind full-length, *E. coli*–expressed HIS_6-Ypp1 (Fig. 2 D). The C terminus of Stt4, which embodies the lipid kinase unique domain and the catalytic lipid kinase domain, did not interact with Ypp1. Interestingly, there are no recognizable structural motifs within the N terminus even though this region of Stt4 is critical for yeast viability; truncations lacking just the N-terminal 135 amino acids fail to localize to the PM or rescue *stt4Δ* cells (unpublished data).

YPP1 and STT4 cooperate to positively maintain PtdIns4P levels

Thus far, our data suggest that Stt4 and Ypp1 directly interact within the PIK patch. We next tested the role for Ypp1 in regulating the kinase activity of Stt4. Our first approach looked at the genetic interaction of mutant alleles of *ypp1* in combination with the *stt4-4* mutant (Audhya et al., 2000). We developed *ypp1* temperature-conditional alleles with compromised growth at elevated temperatures. Seven clones of varying strength, *ypp1-1–7*, were selected based on the extent of their growth disparity at 26 and 37°C. These *ypp1* mutant alleles were each carried on plasmids in the *ypp1Δ* background as described in the Materials and methods.

Our current study utilizes the strongest of these alleles, *ypp1-7*, in combination with the *stt4-4* mutant strain to detect synthetic growth defects. The *ypp1-7* allele, which exhibited strong growth at 26°C, is dead at 37°C (Fig. 3 A). We dissected >20 tetrads generated from diploids with a deleted chromosomal copy of *stt4* and *ypp1* but carrying *stt4-4* and *ypp1-7* on plasmids. We failed to isolate a single mutant strain with the *stt4-4 ypp1-7* combination. The synthetic lethality of the combined mutant alleles suggests the two gene products function in parallel pathways or the same pathway. Additionally, we found that overexpression of *YPP1* from a 2µ plasmid could not rescue the growth defect of *stt4-4* at 37°C (Fig. 3 A, bottom right); however, overexpression of the *STT4* gene from a 2µ plasmid mildly rescues the growth defect of *ypp1-7* at 37°C (Fig. 3 A, top right).

We next addressed Ypp1's effect on Stt4-mediated PtdIns4P synthesis by measuring PIP levels in yeast lacking the Ypp1 protein. Using the *YPP1* clone from the previously characterized yTHC (yeast Tet-promoters Hughes Collection), we were able to significantly diminish Ypp1 levels (Hughes et al., 2000; Mnaimneh et al., 2004). The yTHC contains doxycycline-repressible clones from each of the essential yeast genes, allowing effective depletion of the corresponding protein over the course of around 12–24 h. After a 15-h incubation in the presence of

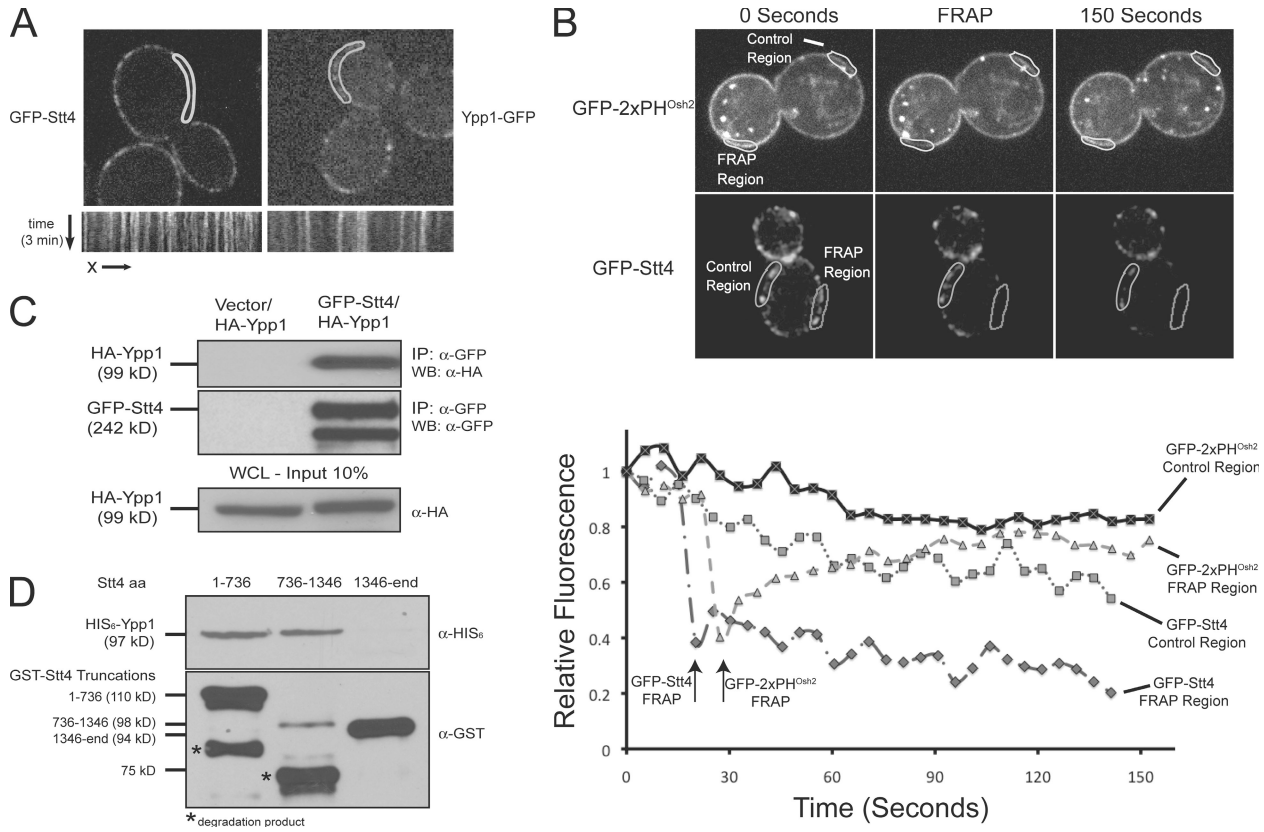

Figure 2. **Stt4 directly interacts with Ypp1 to form a stable complex.** (A) Fluorescent image of GFP-Stt4 (left), Ypp1-GFP (right), and their corresponding kymographs (bottom). A representative section of the cell (the demarcated region in top panels) was examined for its relative movement at the cell membrane. A fluorescent time point of the demarcated region was taken every 5 s over the course of 3 min. The spatial variance of the selected fluorescent region with regard to time is represented in the bottom image. (B) FRAP of the PtdIns4P reporter GFP-2xPH^{Osh2} (top and Video 3, available at http://www.jcb.org/cgi/content/full/jcb.200804003/DC1) and GFP-Stt4 (bottom and Video 2). The white partitions demarcate the regions exposed to high intensity light, a FRAP region, and a control region exposed to normal excitation. The corresponding graph quantifies the fluorescent values with regard to time. (C) Cells expressing HA-Ypp1 and GFP alone or GFP-Stt4 were grown to mid-log phase, lysed, and incubated with an anti-GFP antibody. Coimmunoprecipitated proteins were detected with an anti-HA antibody. The relative abundance of coimmunoprecipitated HA-Ypp1 is shown in the top panel compared with a sample of the input from the whole cell lysate (WCL) in the bottom panel. Note that a small region of the immunoprecipitated GFP-Stt4 is cleaved at the C terminus. (D) Truncation mutants of GST-tagged Stt4 were purified from *E. coli* lysates, immobilized on glutathione beads, and normalized to equal amounts. Beads containing the GST-Stt4 truncations were then incubated for 1 h with lysate from *E. coli* overexpressing HIS$_6$-Ypp1. Protein that bound the GST-Stt4 fragments was probed using an anti-HIS$_6$ antibody. The relative amount of HIS$_6$-Ypp1 that bound each respective GST-Stt4 fragment (top) and the relative amount of the Stt4 fragments that bound the glutathione beads (bottom) are shown. Notice that the primary Stt4 fragment (736–1346) is a C-terminal degradation product missing ~200 amino acids. C-terminal degradation products are marked with an asterisk.

doxycycline, an epitope-tagged Ypp1-HA is no longer detected in cell extracts (Fig. 3 B). Despite low amounts of the essential Ypp1 protein, *tet^o-YPP1* cells remain viable and recover once doxycycline is removed.

We used *tet^o-YPP1* and control strains to measure the relative abundance of the various phosphoinositides by incorporating ^{3}H-labeled myo-inositol into live cells, isolating and deacylating the lipids, and separating the different deacylated inositol species with HPLC. Doxycycline-treated *tet^o-YPP1* cells have PtdIns4P levels reduced to half the relative amount measured in vehicle-treated *tet^o-YPP1* cells (Fig. 3 C). This effect is specific to Ypp1 depletion as treatment of the control strain, *R1158*, with doxycycline showed no decrease of PtdIns4P levels. Consistent with earlier findings regarding inactivation of *stt4*, the downstream lipid PtdIns(4,5)P_2 levels also decrease (Audhya et al., 2000). Similar lipid profiles were observed in experiments using the various *ypp1^{ts}* strains at restrictive temperatures (unpublished data).

Ypp1 selectively impacts the PM pool of PtdIns4P

Our focus turned toward studying steady-state Stt4 activity in the absence of Ypp1. For this, we isolated a bypass suppressor of *ypp1Δ*, the PtdIns 4-phosphatase *SAC1*. We found that yeast lacking *SAC* could bypass deletion of *YPP*. Additionally, *sac1Δ* could bypass *stt4Δ*. The relative growth strength of these various strains demonstrate that the *sac1Δ ypp1Δ* yeast are slightly healthier than *sac1Δ stt4Δ*, implying that the PtdIns 4-kinase may retain some function in the absence of Ypp1 (Fig. 4 A). To further analyze the importance of this finding, we measured PIP levels of each strain.

Deletion of *SAC1*, the primary PtdIns 4-phosphatase for PM-generated PtdIns4P (Guo et al., 1999; Foti et al., 2001), results in a dramatic increase in PtdIns4P levels, tenfold over wild type (Fig. 4 B). However, the double deletion *sac1Δ ypp1Δ* reduces that elevation to roughly twofold wild type. PtdIns4P is further reduced in the *sac1Δ stt4Δ* strain so that it

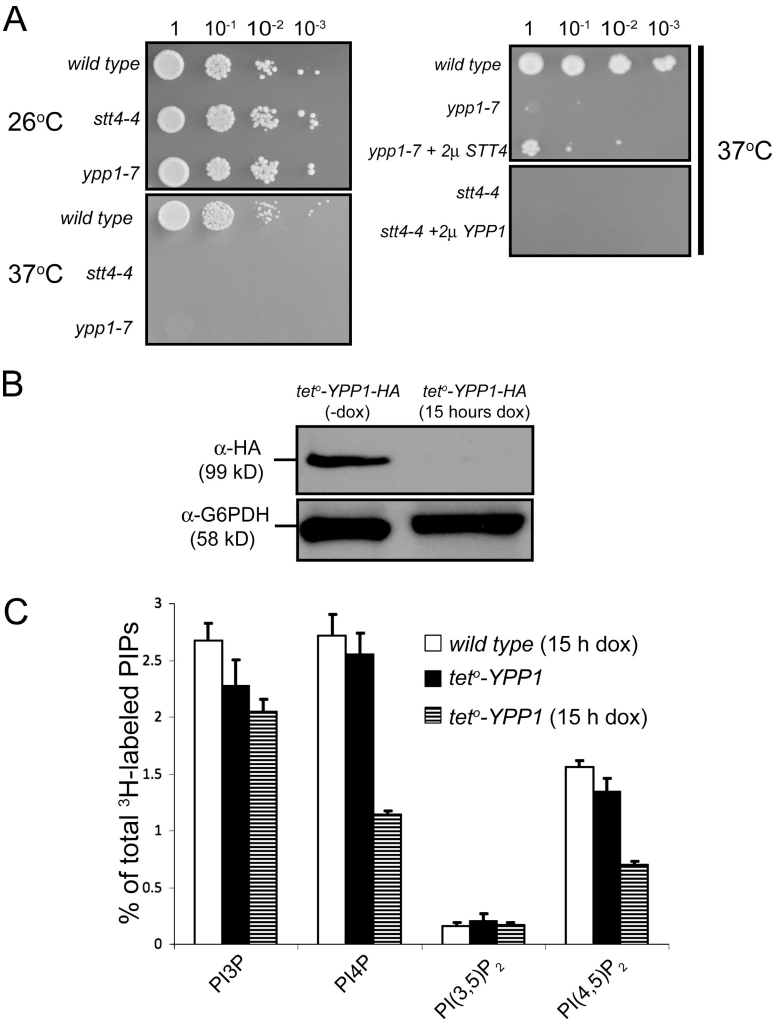

Figure 3. **Ypp1 functions in the PtdIns4P signaling pathway to positively regulate Stt4 kinase activity.** (A) The relative growth capabilities of wild type, *stt4-4*, and *ypp1-7* at 26 (top left) and 37°C (bottom left). The relative growth capability of *ypp1-7* with overexpression of *YPP1* from a 2μ plasmid, plasmid alone (pRS426), or overexpressed *STT4* at 37°C (top right). Similar growth profile of *stt4-4* at 37°C in the presence of vector alone or in the presence of overexpressed *YPP1* (bottom right). (B) Whole cell lysate from *tet°-YPP1-HA* cells grown in the presence or absence of doxycycline were analyzed by Western blot with an anti-HA antibody. The relative abundance of Ypp1-HA under the indicated conditions (top) and the relative abundance of a control protein, G6PDH, from the same lysate (bottom) are shown. (C) Phosphoinositide levels in *tet°-YPP1* cells with and without doxycycline and control *R1158* in the presence of doxycycline. Data are presented as means and SD (error bars) of three independent experiments.

is similar to wild-type levels. Our data imply that Ypp1's impact on PtdIns4P levels comes primarily through Stt4; however, we are unable to completely rule out the possibility that it affects PtdIns4P levels maintained by the other essential PtdIns 4-kinase, Pik1.

We addressed this concern by visualizing the pools of PtdIns4P at the Golgi and PM in various *ypp1* mutant strains. The GFP-tagged tandem Osh2 PH domain has been shown to effectively localize to the two distinct populations of PtdIns4P in the cell, the Pik1-generated Golgi pool and the Stt4-generated PM pool (Roy and Levine, 2004). A disruption in either Pik1 or Stt4 activity redistributes GFP-2xPH^{Osh2} from its wild-type localization (Fig. 4 C, top). In the *stt4^{ts}* mutant at the restrictive temperature, the PM pool of PtdIns4P disappears, whereas under similar conditions in the *pik1^{ts}* mutant the Golgi pool of PtdIns4P disappears. We again used the yTHC *tet°-YPP1* yeast strain to study the localization of GFP-2xPH^{Osh2} upon Ypp1 depletion. In the absence of doxycycline, when Ypp1 is present near normal levels, the localization of GFP-2xPH^{Osh2} was similar to wild type (Fig. 4 C). After 20 h of doxycycline treatment, however, in which the Ypp1 protein has been depleted, the GFP-2xPH^{Osh2} is absent from the PM. This implies that, without Ypp1, PtdIns4P is no longer generated at the PM. Similar results were seen in *sac1Δ ypp1Δ* (unpublished data) confirming the loss of PtdIns4P at the PM in the absence of Ypp1.

An Stt4–Ypp1 complex coordinates PIK patch signaling at the PM

We next analyzed the organization of the PM Stt4 PIK patch. We asked if Ypp1 recruits Stt4 to the PM and/or structurally organizes Stt4 to regulate PtdIns4P metabolism. We detected very low amounts of GFP-Stt4 with either Western blot or fluorescence microscopy in the *sac1Δ ypp1Δ* strain compared with wild type or *sac1Δ*. Therefore, we hypothesized that Ypp1 may be required for the stability of Stt4. We determined that attenuation of Ypp1 levels in the *tet°-YPP1 GFP-STT4* strain caused a corresponding decrease of GFP-Stt4 (Fig. 5 A). Within 9 h, GFP-Stt4 decreased to <10% its initial levels and is barely visible by 16 h. Therefore, we found it very difficult to assess Stt4 distribution in the absence of Ypp1.

To avoid this problem, we monitored GFP-Stt4 localization at various time points after the addition of doxycycline to *tet°-YPP1 GFP-STT4* yeast. This allowed us to study the redistribution of Stt4 as the Ypp1 protein was steadily diminished. After 9 h of doxycycline-induced Ypp1 depletion, GFP-Stt4

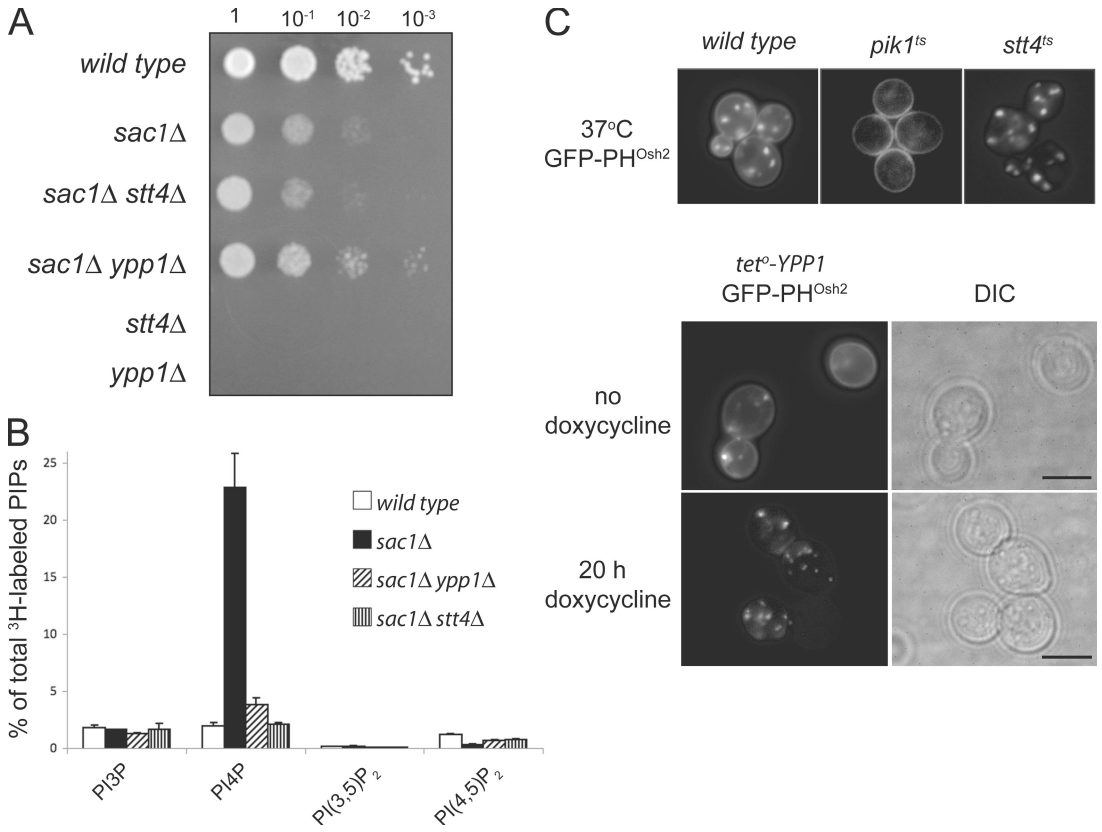

Figure 4. **Deletion of *SAC1* bypasses *ypp1Δ* or *stt4Δ*.** (A) Relative growth profiles of wild type, *sac1Δ*, *sac1Δ stt4Δ*, *sac1Δ ypp1Δ*, *stt4Δ*, and *ypp1Δ* at 26°C. (B) Phosphoinositide levels of wild type, *sac1Δ*, *sac1Δ stt4Δ*, and *sac1Δ ypp1Δ*. Data are presented as means and SD (error bars) of three independent experiments. (C) Cellular localization of the PtdIns4P reporter GFP-2xPH^{Osh2} in wild type, *pik1^{ts}*, and *stt4^{ts}* (top) at the restrictive temperature. (bottom) The fluorescent localization of GFP-2xPH^{Osh2} in *tet^{o}-YPP1* grown in the presence (bottom) or absence (top) of doxycycline for 20 h. Bars, 4 µm.

delocalized from PM PIK patches to the diffuse cytoplasm (Fig. 5 B). Similarly, in *tet^{o}-STT4 GFP-YPP1* (Fig. 5 B), the addition of doxycycline resulted in redistribution of GFP-Ypp1 to the cytoplasm. These results were also observed using *sac1Δ stt4Δ GFP-YPP1* (unpublished data). We conclude that Ypp1 and Stt4 rely on each other to maintain their localization such that recruitment and stability of the PIK patch at the PM depends on an intact Stt4–Ypp1 complex.

Can Ypp1 organize into PIK patches in the absence of Stt4? This question was addressed by artificially targeting Ypp1 to the PM in the absence of Stt4 and studying PIK patch formation. We fused a palmitoylation signal (the first 28 amino acids of Psr1) to the N terminus of full-length GFP-Ypp1 (Siniossoglou et al., 2000). Although this construct failed to rescue *ypp1Δ* cells, it localized similarly to Ypp1 in a wild-type background (Fig. 5 C, top left) and colocalized with mCherry-Stt4 (Fig. S3, available at http://www.jcb.org/cgi/content/full/jcb.200804003/DC1). The absence of Stt4, however, in a *sac1Δ stt4Δ PSR1$^{1-28}$-GFP-YPP1* released Ypp1 from the wild-type cortical PIK patches to a uniform PM distribution. The inverse experiment using *sac1Δ ypp1Δ PSR1$^{1-28}$-GFP-STT4* failed to generate any significant fluorescent signal or maintain any significant protein levels as determined by Western blot. We conclude that Ypp1 is necessary to structurally stabilize Stt4, which in turn allows the complex to organize and be recruited to the PM.

An Stt4–Ypp1 complex forms the core of the PIK patch

We used differential centrifugation to fractionate the various subcellular components of yeast to compare relative PIK patch densities with known cellular components. HA-Ypp1 fractionates into the membrane-associated P100 fraction in a wild-type background (Fig. 6 A). However, deletion of *STT4* in the *sac1Δ* background completely redistributes HA-Ypp1 from P100 fraction to the S100 fraction, indicating that its normal distribution to membrane-bound structures depends on Stt4 (Fig. 6 A, right). We collected this soluble fraction and determined the relative size of a Ypp1 protein complex by measuring its elution from a Superdex S300 column in the absence of Stt4. Soluble HA-Ypp1 (99 kD) from the *stt4Δ sac1Δ* strain was stable and eluted in several fractions with a peak corresponding to a molecular mass of 150 kD (Fig. 6 B). The fast protein liquid chromatography (FPLC) elution profile suggests that Ypp1 may dimerize or bind to other PIK patch-associated components.

We tested Ypp1's capability to dimerize/oligomerize in yeast extracts. Coimmunoprecipitation of HA-Ypp1 with GFP alone, GFP-Ypp1, or GFP-Stt4 demonstrates that HA-Ypp1 interacts well with both GFP-Stt4 and GFP-Ypp1 compared with GFP alone (Fig. 6 C). To test if the interaction between HA-Ypp1 and GFP-Ypp1 is direct or indirect through Stt4, we repeated the experiment in the *sac1Δ stt4Δ* background. In *stt4Δ sac1Δ* yeast lysates, HA-Ypp1 no longer coimmunoprecipitates

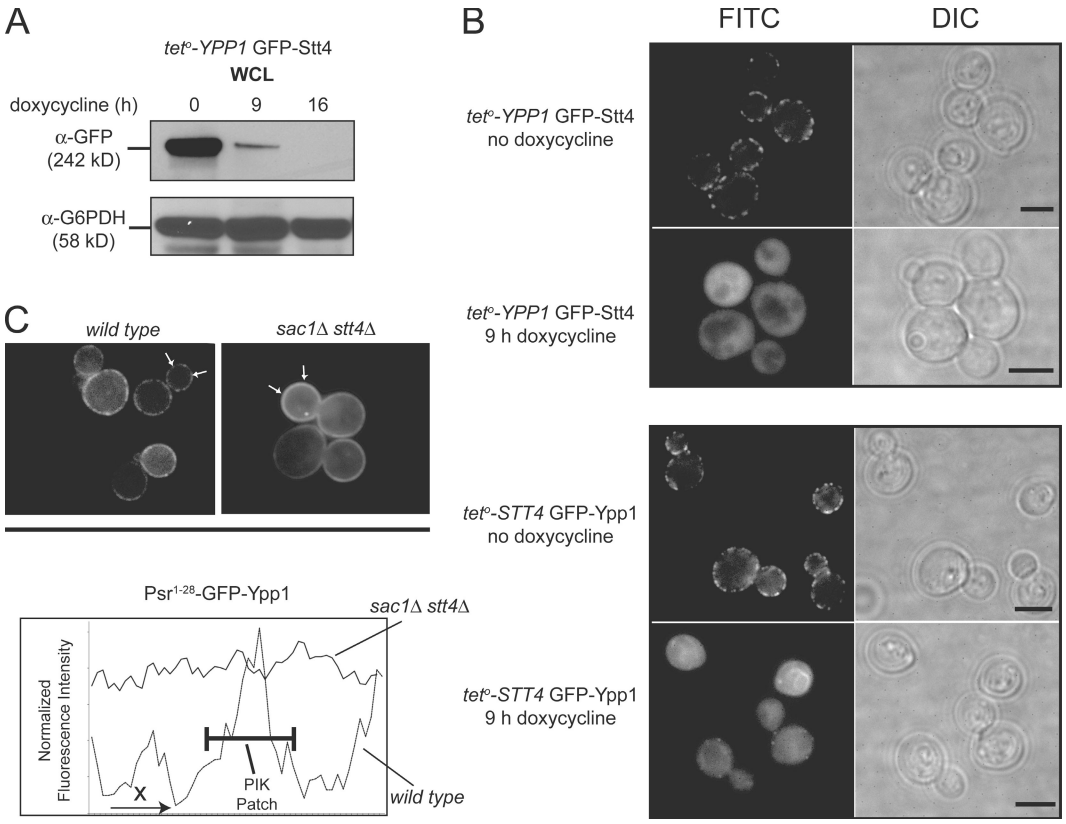

Figure 5. **Stt4 and Ypp1 are codependent for proper localization and organization into PIK patches at the PM.** (A) Relative abundance of GFP-Stt4 after doxycycline treatment in *tet°-YPP1* cells over the time course of 16 h. The relative abundance of G6PDH is shown as a control. (B) The localization profile of *tet°-YPP1* GFP-Stt4 in the absence (top) or presence (second panel) of doxycycline and the corresponding DIC image. The localization *tet°-STT4* GFP-Ypp1 in the absence (third panel) or presence (bottom) of doxycycline and the corresponding DIC images. Bars, 4 µm. (C) Localization of PM anchored $Psr1^{1-28}$-GFP-Ypp1 expressed under wild-type conditions (left) or in the *sac1Δ stt4Δ* background (right). The graph is the relative fluorescence intensity along the PM within the indicated spatial region. Arrows indicating the start and end of the fluorescent images correspond to the x axis of the graph.

with GFP-Ypp1 compared with lysates in which only Sac1 is deleted (Fig. 6 D). Ypp1's inability to directly interact with itself was confirmed with *E. coli*–purified HIS_6-Ypp1. In the absence of any endogenous binding partners, the FPLC elution profile of purified HIS_6-Ypp1 was consistent with a monomer (Fig. 6 E). Therefore, the Ypp1 oligomer requires Stt4. Additionally, the high molecular mass elution profile of HA-Ypp1 isolated from yeast lysates (Fig. 6 B) indicates that HA-Ypp1 has other soluble binding partners in the absence of Stt4.

The rolling blackout (RBO) yeast homologue Efr3 recruits the PIK patch to the PM

Our results indicated that Ypp1 played an essential role in stabilizing Stt4 in the PM PIK patch. However, because neither Stt4 nor Ypp1 contain a recognizable membrane-targeting motif, we predicted that there were additional components critical for PIK patch membrane association. Accordingly, during the course of our Ypp1 characterization, a genome-wide protein interaction study uncovered Efr3 as another candidate component of the Stt4 PIK patch (Tarassov et al., 2008). Similar to *STT4* and *YPP1*, we found that *EFR3* is an essential gene (Fig. 7 A). Primary sequence analysis of Efr3 revealed potential homologues in higher eukaryotes, including humans. The best characterized of these is the *Drosophila melanogaster* RBO gene product, a multipass transmembrane protein essential for viability (Faulkner et al., 1998). Recent work has shown the RBO protein to be localized to presynaptic boutons of *Drosophila* neuromuscular junction synapses, where it has been suggested to have an essential role in synaptic vesicle exocytosis (Huang et al., 2004, 2006).

Multiple lines of evidence indicate that Efr3 is a component of the Stt4 PIK patch. First, Ypp1 and Efr3 interact in vitro based on the ability of *E. coli*–purified GST-Efr3 fusions to bind Ypp1-GFP from yeast lysates. Full-length Efr3 and a C-terminal fragment of Efr3 (amino acids 340–782) can efficiently associate with Ypp1-GFP (Fig. 7 B). Second, as assessed by subcellular fractionation of yeast lysates Efr3-GFP was present in pellet fractions (20% in P13 and 80% in P100) similar to the PIK patch component Ypp1 (Fig. 6 A and Fig. 7 C). Third, Efr3-GFP localizes at PIK patch sites as determined by colocalization with Ypp1-mCherry (Fig. 7 D).

Next, we addressed whether Efr3 functions in PtdIns4P synthesis and Stt4 PIK patch recruitment to the PM. For this, we generated a temperature-conditional mutant allele (see Materials and methods), *efr3-1*, which was unable to grow at the restrictive temperature of 38°C (Fig. 8 A). PtdIns4P levels were then determined at the nonpermissive temperature. Temperature-sensitive *efr3-1* cells displayed reduced PtdIns4P levels as compared with wild-type *EFR3* cells (Fig. 8 B).

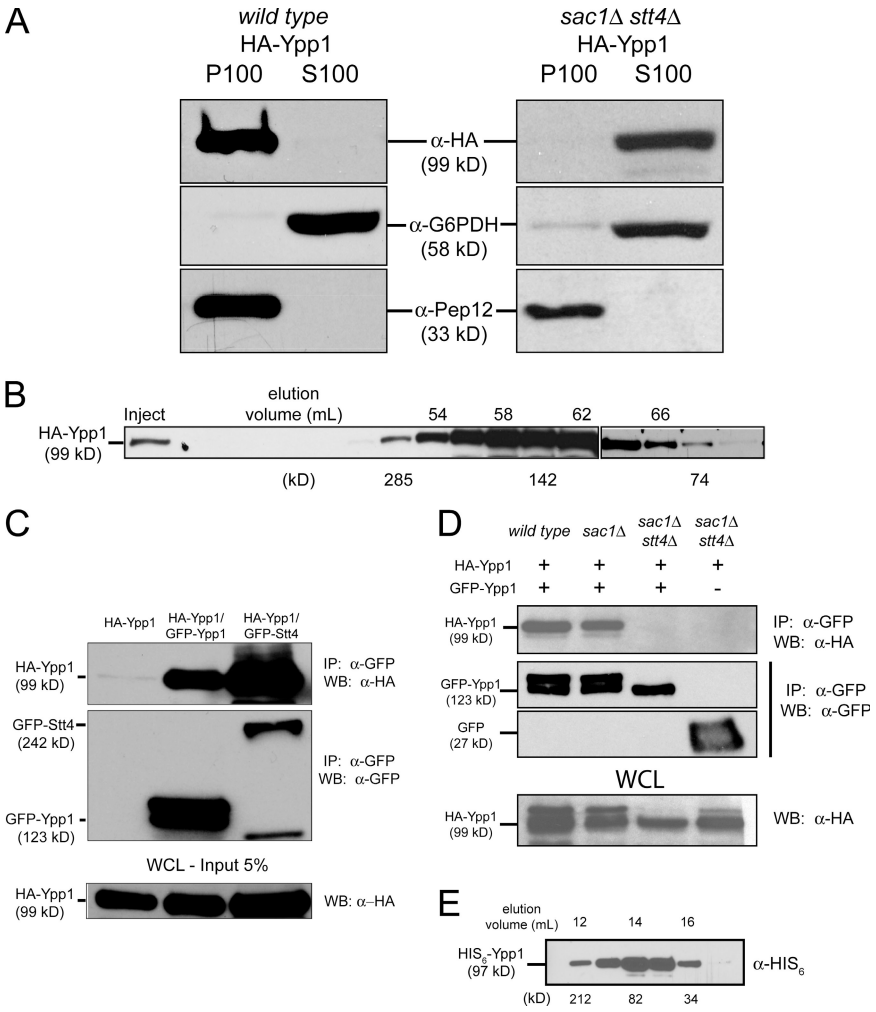

Figure 6. **Stt4 stabilizes Ypp1 molecules on a membrane-bound fraction of the cell.** (A) Subcellular fractionation of cells expressing HA-Ypp1 (left) in a wild-type background and HA-Ypp1 distribution in the absence of *SAC1* and *STT4* (right). Protein component fractions in the pellet (P100; rcf of 100,000) or soluble (S100; soluble portion) fractions. Fractionation of G6PDH (soluble) and Pep13 (membrane-tethered Golgi component) are shown as controls. (B) FPLC elution profile of HA-Ypp1 isolated from the S100 portion of *sac1Δ stt4Δ* cells (top). Fractions were collected at the indicated elution volumes, separated by SDS-PAGE, and detected using an anti-HA antibody. The molecular mass corresponding to each elution is indicated below the blot. (C) Coimmunoprecipitation of HA-Ypp1 from yeast lysate that coexpressed GFP alone, GFP-Ypp1, or GFP-Stt4. (D) Coimmunoprecipitation of HA-Ypp1 with GFP-Ypp1 in the wild type, *sac1Δ*, and *sac1Δ stt4Δ* background. (E) FPLC sizing of *E. coli*–expressed and purified HIS_6-Ypp1 using a Superdex 200 analytical column.

The depressed PtdIns4P appears specific to the PM pool because the PtdIns4P reporter GFP-2xPH^{Osh2} persists at the Golgi but is depleted from the PM in *efr3-1* cells (Fig. 8 C). To assay the impact of Efr3 on PIK patch distribution, we placed *EFR3* under the control of a doxycycline-repressible promoter (*tet^o-EFR3*) to selectively deplete expression of Efr3 in yeast harboring a GFP-tagged PIK patch component, Stt4 or Ypp1. Treatment of the *tet^o-EFR3* GFP-Stt4 strain with doxycycline for 12 h resulted in mislocalization of the lipid kinase to the diffuse cytoplasm (Fig. 8 D). In contrast to Stt4, Efr3-GFP localization was still observed at the PM after depletion of Ypp1 in *tet^o-YPP1* cells treated with doxycycline (Fig. 8 E). However, the patch-like punctate distribution of Efr3-GFP at the PM was reduced (Fig. 8 E). In total, these results suggest that Efr3 mediates PIK patch localization to the PM but also imply that the Stt4–Ypp1 complex could control the clustering of proteins within the PIK patch.

Discussion

PIK patches are oligomeric lipid kinase complexes

PIK patches are large protein complexes consisting of multiple copies of a lipid kinase along with other regulatory proteins oligomerized into a nonuniform punctate arrangement on their substrate membrane. In this work, we focused on PIK patches containing the essential PtdIns 4-kinase Stt4 and identified two essential components critical for Stt4 PIK patch assembly and localization. Previous work had already shown the Stt4 PIK patch to be separate from the PtdIns4P 5-kinase Mss4 PIK patch (Audhya and Emr, 2002) and we now demonstrate that it is also distinct from two other well known PM-associated complexes: actin patches and Pil1-based eisosomes. Kymographic measurements and FRAP experiments demonstrated that Stt4 PIK patches are static with limited exchange of molecules within the patch. These interesting properties coupled to the importance of Stt4-mediated PtdIns4P production at the PM prompted us to seek novel regulatory components of the Stt4 PIK patch. We uncovered two essential proteins. The first was Ypp1, a 95-kD TPR domain–containing protein whose role in the cell had yet to be clearly defined. The second was Efr3, an 89-kD putative membrane protein that shares homology with the *Drosophila* RBO protein.

Our study determined that Ypp1 plays an essential role maintaining PtdIns4P levels at the PM by directly interacting with Stt4 to maintain PIK patch organization and stability of the PtdIns 4-kinase. First, we demonstrated that Ypp1 colocalizes and directly interacts with Stt4 at PIK patch sites on the PM.

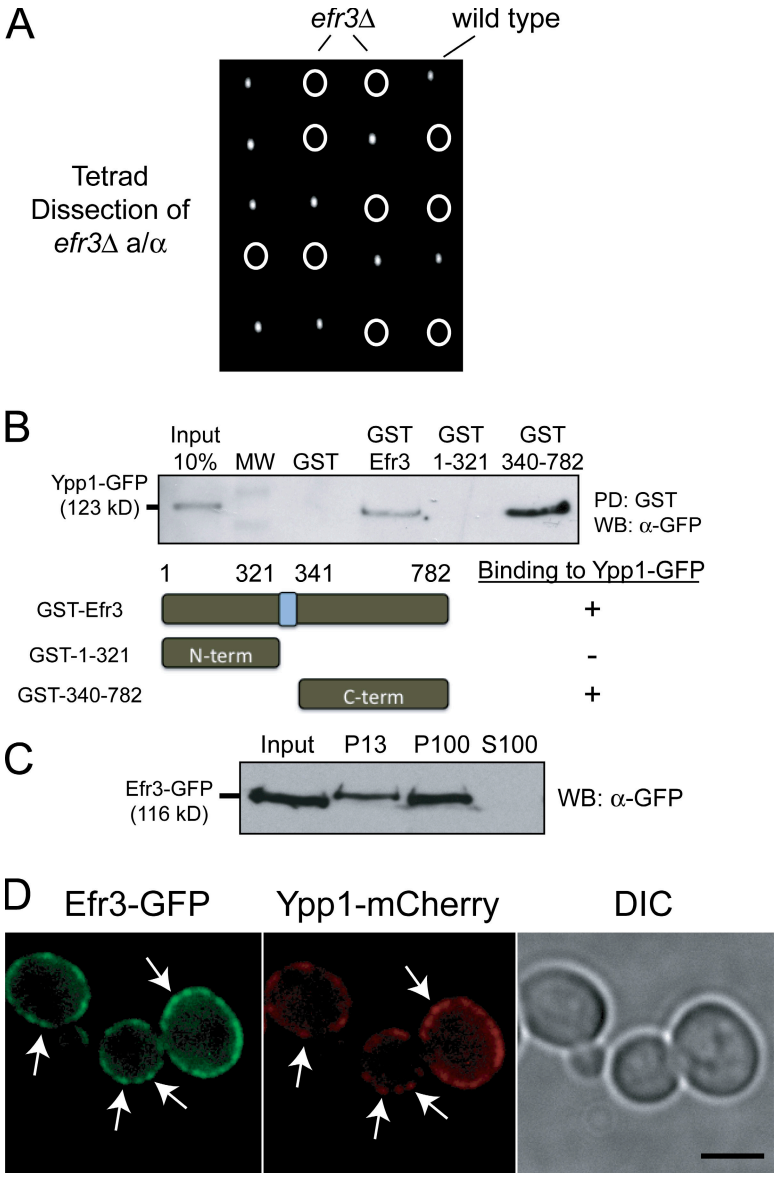

Figure 7. **Efr3 is a component of PIK patches at the PM.** (A) Tetrad dissection of diploid yeast with a deleted chromosomal copy of *efr3*. (B) Full-length and truncation mutants of GST-tagged Efr3 were purified from *E. coli* lysates, immobilized on glutathione beads, and normalized to equal amounts. Beads containing the GST-Efr3 constructs were then incubated for 1 h with yeast lysate expressing Ypp1-GFP. Protein that bound the GST-Efr3 fragments was probed using an anti-GFP antibody. (C) Subcellular fractionation of Efr3-GFP from wild-type cell extracts. (D) Cells coexpressing Efr3-GFP and Ypp1-mCherry were grown at 26°C and examined by fluorescence microscopy. Efr3-GFP localizes to cortical patches on the PM (left) and with a similar distribution as Ypp1-mCherry (right). Arrows on the Efr3-GFP image indicate regions of colocalization. Bar, 4 µm.

Second, our analysis of temperature-sensitive mutant alleles of *stt4* and *ypp1* demonstrated a synthetic lethal interaction, indicating that the two protein products were involved in the same or parallel pathways. Third, using in vitro binding experiments with *E. coli*–expressed proteins, we established that Ypp1 directly binds multiple regions of Stt4. Finally, by placing *YPP1* under the control of a doxycycline-repressible promoter, we showed that in the absence of Ypp1, Stt4 mislocalized to the diffuse cytoplasm and was subsequently degraded causing PtdIns4P levels to drop dramatically at the PM. Similarly, we found that attenuating Stt4 expression caused Ypp1 to delocalize from the PM. However, the Ypp1 protein remained intact and was not degraded. Therefore, we suggest that an intact Stt4–Ypp1 complex is necessary for PM recruitment and subsequent organization into a PIK patch.

Our characterization of Ypp1 and Stt4 indicated that additional factors might control PIK patch organization. During the course of this work, a genome-wide study suggested Efr3 as a candidate Ypp1-interacting protein (Tarassov et al., 2008). We have confirmed Efr3 as a PIK patch component and characterized its role in Stt4 PIK patch assembly. A previous study identified a synthetic lethal genetic interaction between *PHO85* and *EFR3* (PHO eighty five requiring; Lenburg and O'Shea, 2001). Interestingly, Pho85 is a member of the cyclin-dependent kinase family and mammalian Cdk5 has been implicated in PIP metabolism (Lee et al., 2004, 2005). We found that Efr3 is essential, similar to Ypp1 and Stt4. We showed that Efr3 interacts with Ypp1 and colocalizes with Stt4 and Ypp1 at PIK patches on the PM. Additionally, we generated an *efr3^{ts}* allele and demonstrated that at nonpermissive temperatures PtdIns4P levels dropped dramatically at the PM. Finally, we showed that upon depletion of the Efr3 protein, GFP-Stt4 mislocalized from the PM. Importantly, depletion of Ypp1 (or Stt4) did not mislocalize Efr3-GFP from the PM but instead allowed it to adopt a more uniform distribution around the membrane. We propose that Efr3 acts as a PM anchor for Stt4 PIK patches and the Stt4–Ypp1 oligomeric complex stabilizes the distinctive clustering of Stt4 in the PIK patch.

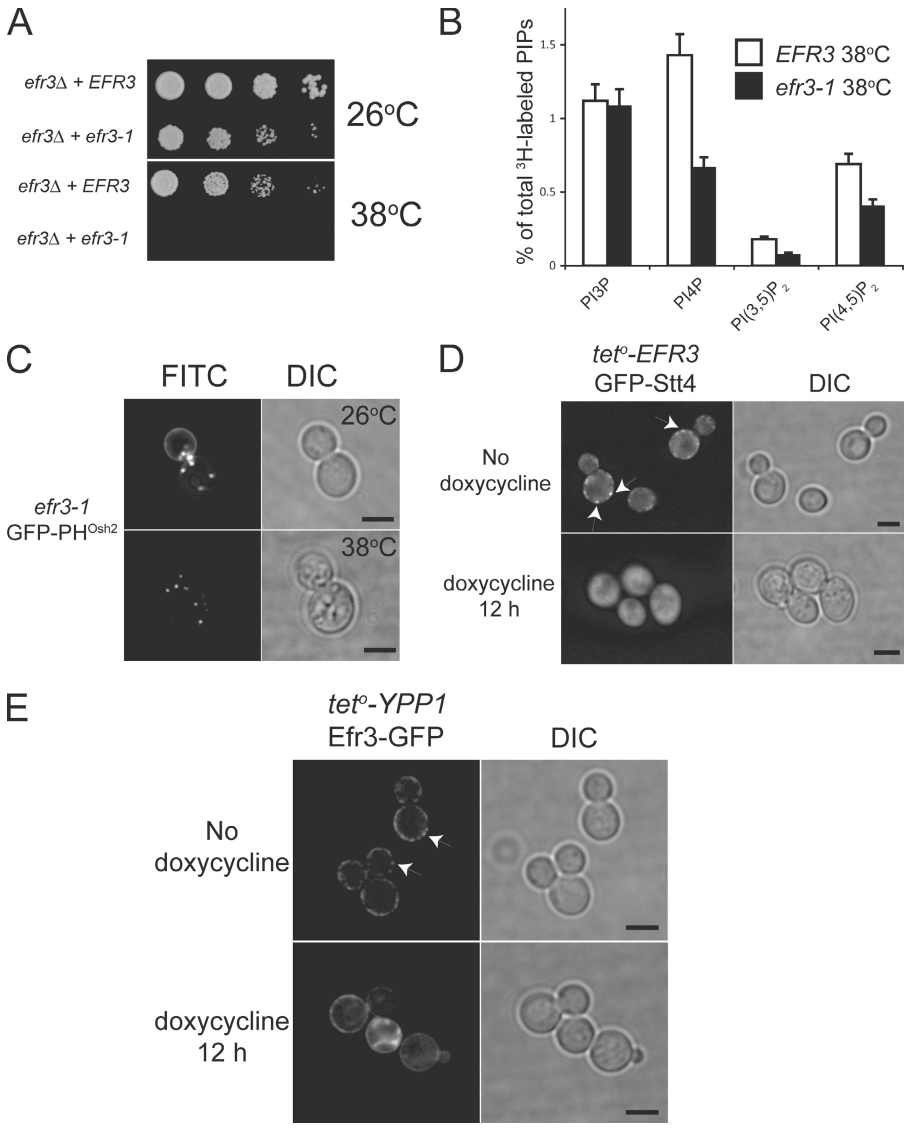

Figure 8. **Efr3 recruits PIK patch components to the PM.** (A) Growth assay of *EFR3* wild type and *efr3-1* temperature-sensitive yeast at 26 and 38°C. (B) Phosphoinositide levels of *EFR3* and *efr3-1* at 38°C. Data are presented as means and SD (error bars) of two independent experiments. (C) Cellular localization of the PtdIns4P reporter GFP-2xPH^{Osh2} in *efr3-1* yeast at the permissive (top) and restrictive (bottom) temperatures. Bars, 4 µm. (D) The localization profile of *tet^{o}-EFR3* GFP-Stt4 in the absence (top) or presence (bottom) of doxycycline and the corresponding DIC image. Arrows indicate PIK patch localization. Bars, 4 µm. (E) The localization profile of *tet^{o}-YPP1* Efr3-GFP in the absence (top) or presence (bottom) of doxycycline and the corresponding DIC images. Arrows indicate PIK patch localization. Bars, 4 µm.

Ypp1 defines a well conserved protein

Ypp1 (YGR198w) is a TPR domain–containing protein with homologues in *Drosophila*, *Mus musculus*, and *Homo sapiens*. TPR domains are a repeating unit of two antiparallel α helices separated by a turn that form a structure resembling a spiraling staircase (Scheufler et al., 2000). These domains are a common structural unit throughout evolution from bacteria to humans and have been shown to be important for directing specific protein–protein interactions (Blatch and Lassle, 1999). The most conspicuous TPR domain–containing proteins are cochaperones, such as Sti1, nonclient binding partners that participate in chaperone-mediated folding of proteins (Prodromou et al., 1999). Ypp1's precise role as a TPR domain–containing protein is consistent with what has already been established for proteins containing this structural feature. As we have demonstrated in this paper Ypp1 is essential for maintaining the integrity of the large PIK patch complex. In the absence of Ypp1, Stt4 is unstable, mislocalizes to the cytoplasm, and is quickly degraded. Therefore, one important role for Ypp1 may be to assist the folding of Stt4 and/or structurally maintain the integrity of the PtdIns 4-kinase within the PIK patch complex.

We were unable to identify a role for Ypp1 independent of Stt4 function, but it is exciting to speculate that the essential Ypp1–Stt4 interaction is maintained throughout evolution. For example, homologues of Ypp1 in higher eukaryotes may also be important for maintaining the structural integrity of protein complexes. For example, *YPP1* has a potential mouse homologue, *TTC7a*, which previous work has found to be essential for normal cell functions. That study determined that a spontaneous retroviral insertion into a TPR domain of *TTC7a* produced a flaky skin (*fsn*) mutation in mice (Helms et al., 2005). The abnormality causes symptoms similar to lupus such as anemia and production of anti-dsDNA autoantibodies. Interestingly, the analogous TPR deletion in Ypp1 yielded a nonfunctional protein unable to bind Stt4 or rescue *ypp1Δ* cells (unpublished data). Helms et al. (2005) speculated that an interaction with a critical TTC7a binding partner is disrupted in *fsn* mice. Could the Stt4 mouse homologue, PtdIns(4)KIIIα, be that protein? Are some mammalian PIK patches no longer stable in the *TTC7a* mouse mutant? Future work in the mouse will be needed to directly address this issue.

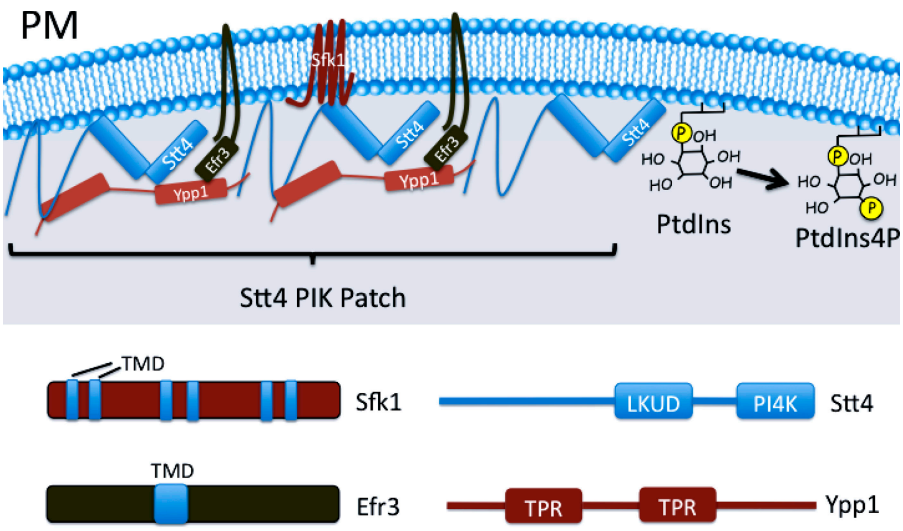

Figure 9. **Organization of Stt4 PIK patches at the PM.** Ypp1 is a multivalent linker of Stt4 molecules ensuring the stability of the lipid kinase and the organization of the PIK patch. Efr3 anchors the Stt4–Ypp1 complex at the PM by binding Ypp1. TMD, transmembrane domain; LKUD, lipid kinase unique domain; PI4K, PtdIns 4-kinase domain.

Efr3, the yeast homologue of *Drosophila* RBO protein, acts as a PIK patch membrane anchor

We also identified Efr3, the yeast homologue of *Drosophila* RBO, as a critical component to maintain PIK patches at the PM. RBO is a multipass transmembrane protein localized to the PM with an essential role in synaptic vesicle trafficking. Based on Efr3's capability to localize to the PM in the absence of other PIK patch components, Efr3 defined a candidate membrane anchor for Stt4 PIK patches. In support of this, a hydrophobicity diagram generated from TMpred software predicts Efr3 to be a one- or two-pass transmembrane protein. Therefore, we propose that Efr3 recruits and anchors the Stt4 PIK patch to the PM. Placing Efr3 in the PM would allow the protein to relay extracellular or membrane activities directly to the Stt4 PIK patch to mediate PtdIns4P metabolism. This idea is supported by the fact that Stt4 activity is important for maintaining cell wall integrity, and Efr3, therefore, may provide a link to the cell wall (Yoshida et al., 1994; Audhya et al., 2000; Audhya and Emr, 2002). Future work will focus on how changes in the extracellular environment or within the membrane, such as cell stress or damage conditions, impact Stt4 PIK patch dynamics and kinase activity.

Can the known function of RBO provide further insight into Efr3's role in the Stt4 PIK patch? RBO has been shown to be important for synaptic vesicle exocytosis based on the observation that synaptic vesicles accumulate at the presynaptic active zone in *rbo*^{ts} mutant neurons shifted to the nonpermissive temperature. The authors attributed the phenotype to a disruption in the balance between synaptic vesicle consumption (exocytosis) and recycling (endocytosis), but favored the idea that RBO functions at the post-docking step of synaptic vesicle exocytosis (Huang et al., 2006). Appropriately, many of the steps involved in synaptic vesicle exocytosis are regulated by lipid composition at the active zone (including the PIP_2 binding proteins synaptotagmin and CAPS) and provide a potential connection to our findings on Efr3's role in PIP dynamics (Osborne et al., 2006).

Previous studies have indicated a link between the secretory and cell polarity pathways in yeast (Aronov and Gerst, 2004; Pruyne et al., 2004) and both Stt4 and Mss4 activity have been shown to be required for cell polarity through the actin cytoskeleton (Audhya et al., 2000; Audhya and Emr, 2002). Besides impacting secretion through actin cytoskeleton dynamics, Stt4 PIK patches may enhance secretion by regulating lipids necessary for exocyst-dependent vesicle fusion. For example, studies have suggested that polarized cell growth is dependent on the exocyst complex through the PtdIns(4,5)P_2 binding components Exo70 and Sec3. Disrupting the PIP binding domain of Exo70 or Sec3 mislocalizes the exocyst complex from the PM and severely impacts secretion (He et al., 2007; Zhang et al., 2008). Future work will investigate potential links between Efr3 activity at the PIK patch and polarized secretion.

A model for PIK patches and their biological function

Fig. 9 provides a model that illustrates how we propose the Stt4 PIK patch organizes at the PM. First, Ypp1 is capable of interacting with at least two separate regions within the N terminus of Stt4 (Fig. 2 D). As a result, Ypp1 could act as a multivalent linker to organize/cluster multiple (~25–30) Stt4 proteins into a PIK patch. Stt4–Ypp1 complexes localize to the PM and further assemble through Efr3 to direct Stt4-mediated PtdIns4P production at the PM. Additional components, such as Sfk1 (Audhya and Emr, 2002), may contribute to the organization and activation of this complex. Because there are potentially other factors associated with regulation of this complex, our future work will be directed toward identifying these components and determining how each factor mediates PIK patch dynamics and PtdIns4P metabolism.

What is the biological significance of forming a large, static Stt4 PIK patch at the PM? Placing multiple PtdIns kinase enzymes into a common complex could permit coordinate activation/inactivation of all the kinases in the complex (PIK patch). This would allow the cell to regulate local levels of PtdIns4P in the PM (activation of some PIK patches while retaining others inactive). However, further experiments are needed to test this idea. Alternatively, the stability of the Stt4 PIK patch suggests they may reside at membrane contact sites linked to the ER.

Table I. **Yeast strains used in this study**

Strain	Genotype	Reference or source
BY4741	*MATa his3*Δ1 *leu2*Δ0 *met15*Δ0 *ura3*Δ0	Mnaimneh et al., 2004
BY4742	*MATα his3*Δ1 *leu2*Δ0 *lys2*Δ0 *ura3*Δ0	Mnaimneh et al., 2004
DBY4	BY4741; *YPP1-GFP::HIS3MX*	This study
DBY16	BY4741; *ypp1Δ::HIS3MX6* carrying pRS415*ypp1-7* (*LEU2 CEN6 ypp1-7*)	This study
DBY21	BY4741; *ypp1Δ::HIS3MX6* carrying pSR54*YPP1* (*LEU2 CEN6 YPP1*)	This study
DBY25	BY4741; *ypp1Δ::HIS3MX6* carrying pBP73-C*YPP1* (*URA3 CEN6 YPP1*)	This study
DBY37	BY4741; *ypp1Δ::HIS3MX6 sac1Δ::KanMX*	This study
DBY42	BY4741; *stt4Δ::HIS3MX6* carrying pRS416*GFP-STT4* (*URA3 CEN6 GFP-STT4*)	This study; Audhya and Emr, 2002
DBY45	BY4741; *stt4Δ::HIS3MX6* carrying pRS415*stt4-4* (*LEU2 CEN6 stt4-4*)	This study; Audhya and Emr, 2002
DBY47	BY4741; *sac1Δ::KanMX*	Winzeler et al., 1999
DBY48	DBY21; *stt4Δ::HIS3MX6* carrying pRS415*stt4-4* (*LEU2 CEN6 stt4-4*)	This study
DBY72	DBY10; *stt4Δ::HIS3MX6* carrying pRS415*stt4-4* (*LEU2 CEN6 stt4-4*)	This study
DBY74	DBY42; *YPP1-mCherry::HIS3MX6*	This study
DBY76	TH2102; *stt4Δ::HIS3MX6* carrying pRS416*GFP-STT4* (*URA3 CEN6 GFP-STT4*)	This study
DBY117	BY4741; *pik1Δ::HIS3MX6* carrying pRS315*pik1-83* (*LEU2 CEN6 pik1-83*)	This study
DBY131	DBY47; *stt4Δ::HIS3MX6*	This study
DBY134	TH2102; *YPP1-HA::HIS3MX6*	This study
DBY294	DBY4; *ABP1-mRFP::HIS3MX6*	This study
DBY298	DBY4; *PIL1-mCherry::HIS3MX6*	This study
DBY417	BY4741; *stt4Δ::HIS3MX6* carrying *pSR54mCherry-Stt4* (*LEU2 CEN6 mCherry-Stt4*) and *pRS416Psr*$^{1\text{-}28}$*-GFP-YPP1* (*URA3 CEN6 Psr*$^{1\text{-}28}$*-GFP-YPP1*)	This study
JBY404	*ade2-1 his3-11,15 leu2-3,112 trp1-1 ura3-1 opi1Δ::LEU2 SEC63-13myc::KAN*^{r} *INO1:LacO128:URA HIS3:LacI-GFP*	Brickner and Walter, 2004
R1158	BY4741; *URA3*::CMV-tTA	Hughes et al., 2000
TH2102	R1158; *pYGR198w*::kanR-tet07-TATA	Peng et al., 2003
TH6139	R1158; *pSTT4*::kanR-tet07-TATA	Peng et al., 2003
DBY454	DBY74; *EFR3-GFP::HISMX3*	This study
DBY482	DBY42; *efr3Δ::HISMX3* carrying *pCM187EFR3* (*URA tet*^{o} *EFR3*)	This study
YCS443	*efr3Δ::HISMX3* carrying *pRS415efr3-1* (*LEU CEN6 efr3-1*)	This study
DBY470	TH2102; *EFR3-GFP::HISMX3*	This study

These contact sites have been hypothesized to be regions through which lipids can easily traffic between closely apposed membranes/organelles (Levine and Loewen, 2006). There is some evidence to support this notion. First, Sac1, the PIP phosphatase that antagonizes Stt4 activity by turning over PtdIns4P at the PM, is an integral transmembrane protein anchored in the ER (Foti et al., 2001). Second, proteomics and genetic screens have identified several potential interactions between Stt4 and ER components (Gavin et al., 2002; Tabuchi et al., 2006). Therefore, Stt4 PIK patch components may be spatially restricted on the PM to sites that are juxtaposed with the ER and these sites could mediate local PIP production and signaling between the two membranes. Future work will explore the possibility that Stt4 PIK patches reside at these potential membrane contact sites and may determine the mechanism for formation and regulation of these contact sites.

Materials and methods

Yeast strains and plasmid construction

A list of all *S. cerevisiae* strains and plasmids used in this study and their genotypes can be found in Table I. The Longtine method (Longtine et al., 1998) was used to introduce gene deletions and epitopes into yeast by homologous recombination. The cloning vectors pRS415 and pRS416 are described in Sikorski and Hieter (1989). The fluorescent fusion vector pBP73-C was a gift from W. Parrish (The Feinstein Institute for Medical Research, Manhasset, NY). The bacterial expression vector pGEX6P-1 used for all the GST constructs is from GE Healthcare and the pET-23d+ vector used for all the HIS_6 constructs is from EMD. The cloning regions of all plasmids were completely sequenced to ensure that no mutations were introduced in the cloning process.

The *GFP-STT4* fusion plasmid has been described previously (Audhya and Emr, 2002). The pRS315*pik1-83* plasmid was subcloned from pRS314*pik1-83* (a gift from J. Thorner, University of California, Berkeley, Berkeley, CA; Hendricks et al., 1999). The pRS415*stt4-4* plasmid has been described previously (Audhya et al., 2000).

Generation of temperature-sensitive *ypp1* and *efr3* alleles

To construct adequate alleles, we used PCR-mediated random mutagenesis of pRS415*YPP1* to generate mutant *ypp1*. These plasmids were subsequently transformed into haploid yeast lacking the chromosomal copy of *YPP1* but carrying a *URA3*$^{+}$ pRS416*YPP1* plasmid. Mutagenized plasmids were selected on 5-FOA plates and then the relative growth capabilities of the various clones were measured at 26 and 37°C. A similar procedure was also used to generate the *efr3-1* temperature-sensitive mutant allele.

Fluorescence microscopy and quantification of fluorescence intensity

Living cells expressing fluorescent fusion proteins were grown in minimal media to an A_{600} of 0.4–0.6. Fluorescence microscopy was performed at 26°C (unless otherwise indicated) in synthetic media. Most images were captured with a microscopy system (DeltaVision RT; Applied Precision, LLC) equipped with a microscope (IX71; Olympus), a PlanApo 100× objective (1.35 NA; Olympus), FITC and rhodamine filters, and a digital camera (Cool Snap HQ; Photometrics) and were deconvolved using softWoRx 3.5.0 software (Applied Precision, LLC). Images for Fig. 1 B and Fig. 2 B were collected with a spinning disc confocal microscopy system (3I; Yokogawa) using a microscope (DMI3000B; Leica) equipped with FITC and rhodamine filters, a 63× (1.40 NA) objective, and a digital camera (QuantEM; Photometrics) and were deconvolved using Slidebook

4.1 (Intelligent Imaging Innovations). The contrast and brightness of the images were further adjusted in Photoshop (Adobe) to give the clearest presentation of the results.

Fluorescence intensity of the GFP (FITC) channel of unprocessed JPEG images was quantified using ImageJ 1.38× (National Institutes of Health). Plot profiles were acquired by drawing a line around the perimeter of the PM and the fluorescence intensity values were exported to Excel 2004 (Microsoft) and normalized.

Pixel-by-pixel analysis was performed using Softworx Data Inspector (Applied Precision, LLC). The Fluorescence Intensity (I_F) of LacI-GFP was measured using a 5 × 5-pixel region of interest (ROI) and subtracted against the nuclear background (5 × 5-pixel ROI of LacI-GFP not present in the dot; Fig. S1 B). I_F of GFP-Stt4 was measured in whole cells using a 5 × 5-pixel ROI and subtracted against background (Fig. S1 B).

In vivo analysis of phosphoinositides

Phosphoinositide levels were analyzed as previously described (Rudge et al., 2004).

For quantitative analyses, dried pellets were resuspended in sterile water and 10^7 cpm of sample was separated on a Partisphere SAX column (GE Healthcare) attached to an HPLC system (Shimadzu Manufacturing) and a 610TR on-line radiomatic detector (PerkinElmer) using Ultima Flo scintillation fluid (PerkinElmer). The HPLC and on-line detector were controlled with EZStart 7.2.1 (Shimadzu) and ProFSA 3.3 (PerkinElmer) software, respectively, with final data analysis taking place in the latter.

Subcellular fractionation

20 A_{600} equivalents of yeast cells were spheroplasted and lysed in 4.3 ml of ice-cold Tris Lysis buffer (50 mM Tris-HCl, pH 7.5, 1 mM EDTA, and 200 mM sorbitol) containing 0.1 mM AEBSF, 0.1 mM chymostatin, 1 µM pepstatin A, and protease inhibitor cocktail (Complete EDTA-free; Roche). 1-ml aliquots of lysates were precleared for 5 min at 500 *g* and were then centrifuged at 13,000 *g* for 10 min at 4°C to generate pellet (P13) and supernatant (S13) fractions. The 1-ml S13 fraction was centrifuged at 100,000 *g* for 1 h at 4°C in an ultracentrifuge (TL-100; Beckman Coulter) to generate the P100 and S100 fractions. Fractions were resolved on a 6% SDS-PAGE gel and immunoblotted.

Protein expression and purification

BL21(DE3)pLys cells (EMD) transformed with protein expression plasmids were grown at 37°C to an A_{600} of 0.4. The bacteria were then shifted to 20°C for 1 h and protein expression was induced by the addition of IPTG to 100 µM for 12 h. For cells expressing GST fusion proteins, cell pellets were resuspended in buffer A (20 mM Hepes, pH 8.0, 250 mM NaCl, 1 mM EDTA 0.5% Tween 20, and 1 mM NaN_3) containing protease inhibitor cocktail and lysed by sonication followed by French Press. Lysates were gently cleared (45 min at 800 *g*) and GST-tagged proteins were purified from the supernatant using glutathione Sepharose 4B (GE Healthcare). After 2 h of incubation, the bead/lysate mix was washed in buffer A three times, and then protein was eluted from the beads with buffer A and 10 mM of reduced glutathione. Proteins were subsequently concentrated and dialyzed into buffer A.

For cells expressing HIS_6 fusion proteins, cell pellets were resuspended in buffer B (20 mM Tris, pH 7.5, 500 mM NaCl, and 20 mM imidazole) with protease inhibitors and prepared similar to GST fusion purification (previous paragraph) except that lysates were cleared by centrifugation (45 min at 13,000 *g*) and purified with Ni-NTA agarose (QIAGEN). The beads were washed extensively and the protein was eluted with buffer B plus 200 mM imidazole.

Sizing of HA-Ypp1 (Fig. 6 B) and HIS6-Ypp1 (Fig. 6 E) was performed on Superdex 300 and 200 analytical columns (GE Healthcare), respectively.

Regulation of gene transcription with doxycycline

Strains from the yTHC (Open Biosystems) were used to regulate expression of essential genes. Typically, the strain of interest was grown up in synthetic media and then diluted to an OD_{600} of 0.01, at which time doxycycline was added to a final concentration of 20 µg/ml. Subsequently, yeast were grown for ~12 h and the abundance of the protein of interest was then measured to determine the relative amount remaining in the cells. Conditions varied slightly between strains tested.

Online supplemental material

Fig. S1 shows coimmunoprecipitation of HA-Stt4 with GFP-Stt4 from yeast lysates and quantification of GFP-Stt4 abundance in PIK patches compared with a LacI-GFP standard. Fig. S2 shows the localization of GFP-Ypp1 compared with other well characterized PM structures. Fig. S3 shows colocalization of $Psr^{1\text{-}28}$-GFP-Ypp1 with mCherry-Stt4. Video 1 is a three-dimensional reconstruction of z stacks from cells expressing GFP-Stt4. Video 2 shows FRAP of GFP-Stt4–based PIK patches. Video 3 shows FRAP of the PtdIns4P reporter GFP-$2xPH^{Osh2}$. Online supplemental material is available at http://www.jcb.org/cgi/content/full/jcb.200804003/DC1.

We are grateful to Jason Yamada-Hanff for excellent technical support through the course of this study. We thank Dr. David Teis for extensive microscopy assistance and critical reading of the manuscript and Dr. Sarah Rue for sharing unpublished plasmids.

S.D. Emr is supported by the Weill Institute for Cell and Molecular Biology at Cornell University. The project described was supported by grant F32GM084567 from the National Institute of General Medical Sciences. The content is solely the responsibility of the authors and does not necessarily represent the official views of the National Institute of General Medical Sciences or the National Institutes of Health.

Submitted: 1 April 2008
Accepted: 14 November 2008

References

Aronov, S., and J.E. Gerst. 2004. Involvement of the late secretory pathway in actin regulation and mRNA transport in yeast. *J. Biol. Chem.* 279:36962–36971.

Audhya, A., and S.D. Emr. 2002. Stt4 PI 4-kinase localizes to the plasma membrane and functions in the Pkc1-mediated MAP kinase cascade. *Dev. Cell.* 2:593–605.

Audhya, A., M. Foti, and S.D. Emr. 2000. Distinct roles for the yeast phosphatidylinositol 4-kinases, Stt4p and Pik1p, in secretion, cell growth, and organelle membrane dynamics. *Mol. Biol. Cell.* 11:2673–2689.

Blatch, G.L., and M. Lassle. 1999. The tetratricopeptide repeat: a structural motif mediating protein-protein interactions. *Bioessays.* 21:932–939.

Brickner, J.H., and P. Walter. 2004. Gene recruitment of the activated INO1 locus to the nuclear membrane. *PLoS Biol.* 2:e342.

D'Andrea, L.D., and L. Regan. 2003. TPR proteins: the versatile helix. *Trends Biochem. Sci.* 28:655–662.

De Camilli, P., S.D. Emr, P.S. McPherson, and P. Novick. 1996. Phosphoinositides as regulators in membrane traffic. *Science.* 271:1533–1539.

Di Paolo, G., and P. De Camilli. 2006. Phosphoinositides in cell regulation and membrane dynamics. *Nature.* 443:651–657.

Faulkner, D.L., T.C. Dockendorff, and T.A. Jongens. 1998. Clonal analysis of cmp44E, which encodes a conserved putative transmembrane protein, indicates a requirement for cell viability in *Drosophila*. *Dev. Genet.* 23:264–274.

Flower, T.R., C. Clark-Dixon, C. Metoyer, H. Yang, R. Shi, Z. Zhang, and S.N. Witt. 2007. *YGR198w* (*YPP1*) targets A30P α-synuclein to the vacuole for degradation. *J. Cell Biol.* 177:1091–1104.

Foti, M., A. Audhya, and S.D. Emr. 2001. Sac1 lipid phosphatase and Stt4 phosphatidylinositol 4-kinase regulate a pool of phosphatidylinositol 4-phosphate that functions in the control of the actin cytoskeleton and vacuole morphology. *Mol. Biol. Cell.* 12:2396–2411.

Gavin, A.C., M. Bosche, R. Krause, P. Grandi, M. Marzioch, A. Bauer, J. Schultz, J.M. Rick, A.M. Michon, C.M. Cruciat, et al. 2002. Functional organization of the yeast proteome by systematic analysis of protein complexes. *Nature.* 415:141–147.

Ghaemmaghami, S., W.K. Huh, K. Bower, R.W. Howson, A. Belle, N. Dephoure, E.K. O'Shea, and J.S. Weissman. 2003. Global analysis of protein expression in yeast. *Nature.* 425:737–741.

Guo, S., L.E. Stolz, S.M. Lemrow, and J.D. York. 1999. SAC1-like domains of yeast SAC1, INP52, and INP53 and of human synaptojanin encode polyphosphoinositide phosphatases. *J. Biol. Chem.* 274:12990–12995.

Hama, H., E.A. Schnieders, J. Thorner, J.Y. Takemoto, and D.B. DeWald. 1999. Direct involvement of phosphatidylinositol 4-phosphate in secretion in the yeast *Saccharomyces cerevisiae*. *J. Biol. Chem.* 274:34294–34300.

Hazbun, T.R., L. Malmstrom, S. Anderson, B.J. Graczyk, B. Fox, M. Riffle, B.A. Sundin, J.D. Aranda, W.H. McDonald, C.H. Chiu, et al. 2003. Assigning function to yeast proteins by integration of technologies. *Mol. Cell.* 12: 1353–1365.

He, B., F. Xi, X. Zhang, J. Zhang, and W. Guo. 2007. Exo70 interacts with phospholipids and mediates the targeting of the exocyst to the plasma membrane. *EMBO J.* 26:4053–4065.

Heck, J.N., D.L. Mellman, K. Ling, Y. Sun, M.P. Wagoner, N.J. Schill, and R.A. Anderson. 2007. A conspicuous connection: structure defines function

for the phosphatidylinositol-phosphate kinase family. *Crit. Rev. Biochem. Mol. Biol.* 42:15–39.

Helms, C., S. Pelsue, L. Cao, E. Lamb, B. Loffredo, P. Taillon-Miller, B. Herrin, L.M. Burzenski, B. Gott, B.L. Lyons, et al. 2005. The Tetratricopeptide repeat domain 7 gene is mutated in flaky skin mice: a model for psoriasis, autoimmunity, and anemia. *Exp. Biol. Med. (Maywood).* 230:659–667.

Hendricks, K.B., B.Q. Wang, E.A. Schnieders, and J. Thorner. 1999. Yeast homologue of neuronal frequenin is a regulator of phosphatidylinositol-4-OH kinase. *Nat. Cell Biol.* 1:234–241.

Honda, A., M. Nogami, T. Yokozeki, M. Yamazaki, H. Nakamura, H. Watanabe, K. Kawamoto, K. Nakayama, A.J. Morris, M.A. Frohman, and Y. Kanaho. 1999. Phosphatidylinositol 4-phosphate 5-kinase alpha is a downstream effector of the small G protein ARF6 in membrane ruffle formation. *Cell.* 99:521–532.

Huang, F.D., H.J. Matthies, S.D. Speese, M.A. Smith, and K. Broadie. 2004. Rolling blackout, a newly identified PIP2-DAG pathway lipase required for *Drosophila* phototransduction. *Nat. Neurosci.* 7:1070–1078.

Huang, F.D., E. Woodruff, R. Mohrmann, and K. Broadie. 2006. Rolling blackout is required for synaptic vesicle exocytosis. *J. Neurosci.* 26:2369–2379.

Hughes, T.R., M.J. Marton, A.R. Jones, C.J. Roberts, R. Stoughton, C.D. Armour, H.A. Bennett, E. Coffey, H. Dai, Y.D. He, et al. 2000. Functional discovery via a compendium of expression profiles. *Cell.* 102:109–126.

Kaksonen, M., C.P. Toret, and D.G. Drubin. 2005. A modular design for the clathrin- and actin-mediated endocytosis machinery. *Cell.* 123:305–320.

Lee, S.Y., M.R. Wenk, Y. Kim, A.C. Nairn, and P. De Camilli. 2004. Regulation of synaptojanin 1 by cyclin-dependent kinase 5 at synapses. *Proc. Natl. Acad. Sci. USA.* 101:546–551.

Lee, S.Y., S. Voronov, K. Letinic, A.C. Nairn, G. Di Paolo, and P. De Camilli. 2005. Regulation of the interaction between PIPKIγ and talin by proline-directed protein kinases. *J. Cell Biol.* 168:789–799.

Lemmon, M.A. 2003. Phosphoinositide recognition domains. *Traffic.* 4:201–213.

Lenburg, M.E., and E.K. O'Shea. 2001. Genetic evidence for a morphogenetic function of the *Saccharomyces cerevisiae* Pho85 cyclin-dependent kinase. *Genetics.* 157:39–51.

Levine, T., and C. Loewen. 2006. Inter-organelle membrane contact sites: through a glass, darkly. *Curr. Opin. Cell Biol.* 18:371–378.

Ling, K., R.L. Doughman, V.V. Iyer, A.J. Firestone, S.F. Bairstow, D.F. Mosher, M.D. Schaller, and R.A. Anderson. 2003. Tyrosine phosphorylation of type Iγ phosphatidylinositol phosphate kinase by Src regulates an integrin–talin switch. *J. Cell Biol.* 163:1339–1349.

Longtine, M.S., A. McKenzie III, D.J. Demarini, N.G. Shah, A. Wach, A. Brachat, P. Philippsen, and J.R. Pringle. 1998. Additional modules for versatile and economical PCR-based gene deletion and modification in *Saccharomyces cerevisiae*. *Yeast.* 14:953–961.

Mnaimneh, S., A.P. Davierwala, J. Haynes, J. Moffat, W.T. Peng, W. Zhang, X. Yang, J. Pootoolal, G. Chua, A. Lopez, et al. 2004. Exploration of essential gene functions via titratable promoter alleles. *Cell.* 118:31–44.

Muhua, L., N.R. Adames, M.D. Murphy, C.R. Shields, and J.A. Cooper. 1998. A cytokinesis checkpoint requiring the yeast homologue of an APC-binding protein. *Nature.* 393:487–491.

Odorizzi, G., M. Babst, and S.D. Emr. 2000. Phosphoinositide signaling and the regulation of membrane trafficking in yeast. *Trends Biochem. Sci.* 25:229–235.

Osborne, S.L., P.J. Wen, and F.A. Meunier. 2006. Phosphoinositide regulation of neuroexocytosis: adding to the complexity. *J. Neurochem.* 98:336–342.

Peng, W.T., M.D. Robinson, S. Mnaimneh, N.J. Krogan, G. Cagney, Q. Morris, A.P. Davierwala, J. Grigull, X. Yang, W. Zhang, et al. 2003. A panoramic view of yeast noncoding RNA processing. *Cell.* 113:919–933.

Prodromou, C., G. Siligardi, R. O'Brien, D.N. Woolfson, L. Regan, B. Panaretou, J.E. Ladbury, P.W. Piper, and L.H. Pearl. 1999. Regulation of Hsp90 ATPase activity by tetratricopeptide repeat (TPR)-domain co-chaperones. *EMBO J.* 18:754–762.

Pruyne, D., L. Gao, E. Bi, and A. Bretscher. 2004. Stable and dynamic axes of polarity use distinct formin isoforms in budding yeast. *Mol. Biol. Cell.* 15:4971–4989.

Roy, A., and T.P. Levine. 2004. Multiple pools of phosphatidylinositol 4-phosphate detected using the pleckstrin homology domain of Osh2p. *J. Biol. Chem.* 279:44683–44689.

Rudge, S.A., D.M. Anderson, and S.D. Emr. 2004. Vacuole size control: regulation of PtdIns(3,5)P2 levels by the vacuole-associated Vac14-Fig4 complex, a PtdIns(3,5)P2-specific phosphatase. *Mol. Biol. Cell.* 15:24–36.

Scheufler, C., A. Brinker, G. Bourenkov, S. Pegoraro, L. Moroder, H. Bartunik, F.U. Hartl, and I. Moarefi. 2000. Structure of TPR domain-peptide complexes: critical elements in the assembly of the Hsp70-Hsp90 multichaperone machine. *Cell.* 101:199–210.

Sikorski, R.S., and P. Hieter. 1989. A system of shuttle vectors and yeast host strains designed for efficient manipulation of DNA in *Saccharomyces cerevisiae*. *Genetics.* 122:19–27.

Simonsen, A., A.E. Wurmser, S.D. Emr, and H. Stenmark. 2001. The role of phosphoinositides in membrane transport. *Curr. Opin. Cell Biol.* 13:485–492.

Siniossoglou, S., E.C. Hurt, and H.R. Pelham. 2000. Psr1p/Psr2p, two plasma membrane phosphatases with an essential DXDX(T/V) motif required for sodium stress response in yeast. *J. Biol. Chem.* 275:19352–19360.

Stefan, C.J., S.M. Padilla, A. Audhya, and S.D. Emr. 2005. The phosphoinositide phosphatase Sjl2 is recruited to cortical actin patches in the control of vesicle formation and fission during endocytosis. *Mol. Cell. Biol.* 25:2910–2923.

Strahl, T., H. Hama, D.B. DeWald, and J. Thorner. 2005. Yeast phosphatidylinositol 4-kinase, Pik1, has essential roles at the Golgi and in the nucleus. *J. Cell Biol.* 171:967–979.

Tabuchi, M., A. Audhya, A.B. Parsons, C. Boone, and S.D. Emr. 2006. The phosphatidylinositol 4,5-biphosphate and TORC2 binding proteins Slm1 and Slm2 function in sphingolipid regulation. *Mol. Cell. Biol.* 26:5861–5875.

Tarassov, K., V. Messier, C.R. Landry, S. Radinovic, M.M. Serna Molina, I. Shames, Y. Malitskaya, J. Vogel, H. Bussey, and S.W. Michnick. 2008. An in vivo map of the yeast protein interactome. *Science.* 320:1465–1470.

Voelker, D.R. 2005. Protein and lipid motifs regulate phosphatidylserine traffic in yeast. *Biochem. Soc. Trans.* 33:1141–1145.

Walch-Solimena, C., and P. Novick. 1999. The yeast phosphatidylinositol-4-OH kinase pik1 regulates secretion at the Golgi. *Nat. Cell Biol.* 1:523–525.

Walther, T.C., J.H. Brickner, P.S. Aguilar, S. Bernales, C. Pantoja, and P. Walter. 2006. Eisosomes mark static sites of endocytosis. *Nature.* 439:998–1003.

Winzeler, E.A., D.D. Shoemaker, A. Astromoff, H. Liang, K. Anderson, B. Andre, R. Bangham, R. Benito, J.D. Boeke, H. Bussey, et al. 1999. Functional characterization of the *S. cerevisiae* genome by gene deletion and parallel analysis. *Science.* 285:901–906.

Yoshida, S., Y. Ohya, M. Goebl, A. Nakano, and Y. Anraku. 1994. A novel gene, STT4, encodes a phosphatidylinositol 4-kinase in the PKC1 protein kinase pathway of *Saccharomyces cerevisiae*. *J. Biol. Chem.* 269:1166–1172.

Yu, J.W., J.M. Mendrola, A. Audhya, S. Singh, D. Keleti, D.B. DeWald, D. Murray, S.D. Emr, and M.A. Lemmon. 2004. Genome-wide analysis of membrane targeting by *S. cerevisiae* pleckstrin homology domains. *Mol. Cell.* 13:677–688.

Zhang, X., K. Orlando, B. He, F. Xi, J. Zhang, A. Zajac, and W. Guo. 2008. Membrane association and functional regulation of Sec3 by phospholipids and Cdc42. *J. Cell Biol.* 180:145–158.